Transport and deposit of oxygen in the wake of an inertial bubble rising in a thin-gap cell

Francisco Felis, Sébastien Cazin, Nicolas Dietrich, Anne-Marie Billet, Karine Loubière, Véronique Roig

Transport and deposit of oxygen in the wake of an inertial bubble rising in a thin-gap cell

Francisco Felis[1,2,3], Sébastien Cazin[3], Nicolas Dietrich[4], Anne-Marie Billet[2], Karine Loubière[2,*], Véronique Roig[3,*]

[1] *Féderation de Recherche FERMAT, CNRS, Toulouse, France*
[2] *Laboratoire de Génie Chimique, Université de Toulouse, CNRS, INPT, UPS, Toulouse, France*
[3] *Institut de Mécanique des Fluides de Toulouse (IMFT), Université de Toulouse, CNRS, Toulouse, France*
[4] *Toulouse Biotechnologie Institute (TBI), Université de Toulouse, CNRS , INRAE, INSA, Toulouse, France*

*Corresponding author(s): roig@imft.fr; karine.loubiere@cnrs.fr

Summary

We explore the transport of oxygen delivered by an inertial bubble rising in a fluid at rest in a vertical confined cell. While the mass transfer has been proved to be enhanced by confinement, there is poor knowledge of the 3D mechanisms of concentration transport in this flow configuration. The residence time in the attached wake and the mixing induced by vortices may affect yields of reaction products and selectivity in chemical reaction systems. It is therefore necessary to discuss the 3D transport of concentration, and this is the focus of this contribution.

Keywords: Reactive multiphase flow, Confined inertial bubble, 3D wakes, Mass transfer, transport of concentration

Introduction

New experimental results are reported for oxygen mass transfer at the interface of an isolated bubble rising in liquid at rest, the bubble being confined in a vertical thin-gap cell of thickness w smaller than the capillarity length. Considered bubbles have a diameter d greater than w and therefore look like 'pancakes' separated from the walls by thin liquid films. The flow regime is inertial, and there exists a strong coupling between the bubble motion and its wake dynamics (Roig et al., 2012; Filella et al., 2015). Previous studies have already shown that such flow configuration can intensify mass transfer (Roudet et al., 2017 ; Felis et al., 2019 ; Zhang et al., 2020 ; Laurini et al., 2023). This mass transfer leads to the transport of oxygen in the flow perturbation generated by the bubble motion. Understanding the gas-liquid interactions in bubble wakes is crucial for discussing yield and selectivity when implementing a reaction in which a gaseous reactant is transferred through the fluid interfaces (Khinast, 2001; Kursula et al., 2022). Therefore, a focus is here paid on the role of the 3D velocity field in the oxygen transport through the liquid. The questions that are addressed concern: (i) the characterization of the 3D velocity field in the vicinity of the bubble that directly acts on mass transfer; (ii) the occurrence of contrasted mass transfers in the films and at the bubble interface surrounded by high-Reynolds number external flow; (iii) the locations of intense mass transfer sources and the times at which they are activated; (iv) the modes of concentration transport before oxygen is finally deposed in the far wake of the bubbles.

Experimental and Numerical Methods

Two similar experimental set-ups have been used for this study either to investigate mass transfer and bubble kinematics or to perform tomo-PTV 4D measurements. They both consisted in a planar vertical thin-gap cell filled with a liquid initially at rest consisting in water for tomo-PTV experiments and in a specific reactive aqueous solution for mass transfer characterization.

For mass transfer investigation, the experimental set-up is the same as in Felis et al. (2019) and Laurini et al (2023). The thin-gap cell was filled with an oxygen-free reactive aqueous solution and its height and horizontal width were $H = 400$ mm and $W = 200$ mm. The width of the gap was $w = 1.062$ mm ± 0.005 mm. A bubble of pure oxygen was released at the bottom of the cell using a burst valve. It rose freely through the cell and transferred some oxygen without changing its volume. In any case, the volume of the bubble was large enough so that it was flattened in between the walls of the cell and adopted in-plane motions while rising. An imaging system based on shadowgraph technique was used to follow the path of the bubble, its in-plane shape oscillations and the gap-averaged oxygen concentration released around it. The cell was thus illuminated from behind with a white LED backlight panel collimated white LED backlight panel (PHLOX, 400×200 mm²) and a 16-bit sCMOS PCO Edge 2560×2160 px camera equipped with a 50 mm 1:12 Nikon lens was placed in front of the cell. The equivalent diameter of the bubble, d, was associated to the bubble in-plane projected area. As liquid phase, a reactive solution was considered for this study (see Dietrich et al., 2013 or Yang et al., 2016). It consisted in an aqueous solution of resazurin dye which physico-chemical properties differed only slightly from the ones of pure deionised water. In oxygen-free atmosphere, this solution was transparent, and when it was in contact with oxygen a pale pink color appeared due to the fast chemical reaction between oxygen and the dye. This reaction was

reversible (the back reaction was very slow, i.e. few minutes) and occurred in presence of glucose and sodium hydroxide. With an adequate calibration of the grey levels delivered by the camera and knowing the stoichiometry of the reaction, it was possible to describe the field of 'equivalent' oxygen concentration averaged through the gap of the cell. The diffusivity of oxygen in this mixture was $D = 3.2\ 10^{-9}$ m^2/s.

We also performed detailed experiments to explore the 3D character of the velocity field in the liquid phase around the confined bubble. They were performed in a cell of identical gap-width but larger in-plane dimensions (oxygen concentration and liquid velocity measurements could not be performed simultaneously). A 4D Lagrangian Particle Tracking Velocimetry (PTV) experimental technique was used to explore the structure of the liquid velocity field so as to decipher the complexity of the mass transfer and the transport of concentration. Particle tracks (positions) and individual velocities were calculated using the Shake-The-Box (STB) method as in Pavlov et al. (2021).

We present here results obtained for two different bubbles which characteristics are reported in Table 1. For the largest Archimedes number *Ar*, the bubble rose steadily and adopted a hemi-cylindrical shape in both types of measurements. For *Ar* =2660, the bubble had an oscillating motion path and presented shape oscillations.

For the 4D-PTV post-processing, we took advantage of the steady rising velocity of one of the bubbles, where the reference frame was changed to the bubble's by subtracting its captured velocity to the particles' positions. Following this, an ensemble PTV was considered by superimposing all particle tracks to increase resolution. These tracks were then individually smoothed using a long-pass filter in time, and the whole ensemble was interpolated into a regular grid using a gaussian-kernel radial basis function. From this, a smooth 3D vector field could be visualized like in Figure 2, and the generation of streamlines like in Figure 3.

Table 1. Bubbles characteristics ($Ar = \sqrt{gd}d/\nu_L, Bo = \rho_L g d^2/\sigma$) where g is gravity acceleration, ν_L kinematic viscosity of the liquid and σ the interfacial tension.

Bubbles for mass transfer		
Ar	**Bo**	**d/w**
4670	26	14.1
2660	12.1	9.7
Bubbles for tomo-PTV 4D		
Ar	**Bo**	
4630	30	14

Results and Discussion

Mass transfer and concentration transport around a large bubble rising steadily

Figure 1 shows the gap-averaged concentration of oxygen around the large bubble. It consists in a large ribbon of orange color (~ 0.6 mgO_2/L) delivered by the thin liquid films superposed to a less important amount of oxygen that is transferred at the upstream part of the bubble and that surrounds the bubble before being concentrated in the central part of the wake. The ribbon originates from the films because (i) it is aligned with the transverse extend of the bubble and (ii) examination of the movies shows that this concentration part does not move at all as it stays in the vicinity of the walls. The mass transfer at the front of the bubble leads to a region colored in blue (~ 0.2 mgO_2/L) that is too thick to be a diffusive mass boundary layer. Indeed, it is associated to the transport of concentration in horseshoe vortices preceding the bubble, as proved by the Tomo-PTV exploration. By plotting the transverse view of the measured velocity field, Figure 2 clearly shows the presence of two horseshoe vortices in front of the bubble. It also reveals that the wake consists in a complex 3D flow with two superposed recirculating zones. The bubble is therefore followed by four recirculating zones constituting its attached wake.

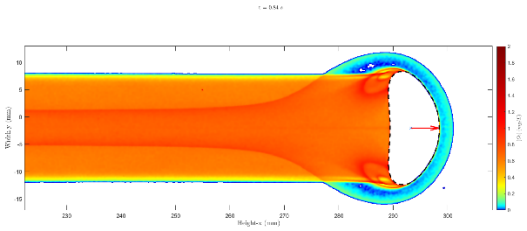

Figure 1: Measured gap-averaged concentration of oxygen around a large bubble (*Ar* =4670, *Bo* = 26) (The bubble rises from left to right).

Figure 2: Description of the 3D velocity field around the large bubble (*Ar* = 4630, *Bo* =30) by tomo-PTV technique. Transverse view of the liquid velocity vectors in front of the bubble and in its near wake in the central plane (the height of the figure is *w* = 1 mm. The bubble is represented arbitrarily in grey color. Reference frame is the one of the bubble. The bubble front is on the right side.).

Figure 3 shows some fluid streamlines around the same bubble that converge in the middle gap plane in the far wake. Views in the cell plane (upper view) and in the gap plane (lower view) are reported. The bundle of streamlines that touches the bubble interface can be visually distinguished from the one that does not touch it, thus being not fed with concentration by interfacial mass transfer. The similarity between the curvatures of the streamlines touching the interface in the cell plane and the curvature of the concentration field in Figure 1 indicates the origin of the concentration overlaying the ribbon. It comes from mass

transfer in the high-Reynolds number surrounding flow.

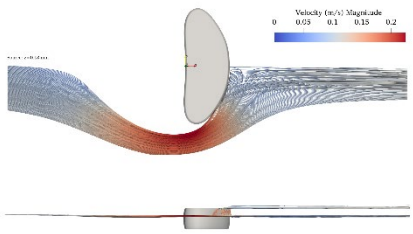

Figure 3: Description of the 3D velocity field around the large bubble (*Ar* = 4630, *Bo* =30) by tomo-PTV technique. Streamlines viewed from the direction perpendicular to the cell (upper view) and from an in-plane direction (lower view).

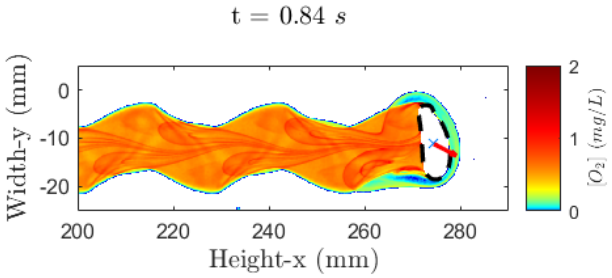

Figure 4: Instantaneous field of gap-averaged concentration of oxygen around an oscillating bubble (Ar =2660, Bo = 12.1)

Mass transfer and concentration transport around an oscillating bubble

As revealed in Figure 4, the instantaneous concentration field around the oscillating bubble also consists in a ribbon of oxygen delivered by the thin liquid films and an added distribution in a vortex array coupled to horseshoe vortices preceding the bubble. The ribbon coming from the films is periodic as it is deposed at the wall by an oscillating bubble. It is periodically modulated by concentration patterns due to either the oscillating films dynamics or to the possible presence of heterogeneities in the film (such as presence of surface active agents or thickness variations). As the film has not been explored, it is not possible to conclude about the origin of this periodic pattern.

The contrasted periodic array of concentration transported by the elongated vortices trailing the bubble is also quite original. Indeed, the mechanistic scenario leading to such periodic array in the wake is the following. It results from both the curvature, tilting and stretching of the horseshoe vortices and the local periodic injection of oxygen from the equator of the oscillating bubble where a localized shear layer develops and sheds supplementary vorticity. While the tomo-PTV exploration of the 3D velocity field around the bubble is still hard to obtain, the whole scenario is compatible with the previous characterizations of the vortex dynamics, especially with the dynamics of their release (Filella et al., 2015). An observation of a movie of the concentration field indicates that the ribbon and its periodic patterns do not move at all. It also reveals that the array of released vortices has a short life-time for movements. At around 6*d* form the bubble, the motion is dampened by the confinement and periodic patterns of concentration are deposed in the cell. They survive until the characteristic back reaction happens, that is for a few minutes after the bubble passage.

Conclusions

The knowledge of gap-averaged concentration field and of the 3D dynamics of the liquid around confined bubbles allows identification of main contrasted mechanisms involved in concentration transport around an isolated bubble rising in a liquid at rest in a confined cell. This study reveals the strong role of horseshoe vortices in this transport, but also that behind bubbles, two contrasted regions are fed by mass transfer either in the thin liquid films or around the free periphery of the bubble that does not face the walls. This leads to a double periodic deposit of oxygen at the rear of these confined bubbles. A more precise examination of the concentration field will allow us to discuss the combination of concentration issued from the front part of the bubble and from punctual release of oxygen in the vortices that detach in the shear layer developing at the equator of the bubble.

References

Dietrich, N., Loubière, K., Jimenez, M., Hébrard, G., Gourdon, C., 2013, A new direct technique for visualizing and measuring gas-liquid mass transfer around bubbles moving in a straight millimetric square channel. Chemical Engineering Science, 100:172–182.

Felis F., Strassl F., Laurini L., Dietrich N., Billet A-M., Roig V., Herres-Pawlis S. Loubière K., 2019, Using a bio-inspired copper complex to investigate reactive mass transfer around an oxygen bubble rising freely in a thin-gap cell, Chem. Eng. Sci. 207 pp. 1256–1269.

Filella A., Ern P., Roig V., 2015, Oscillatory motion and wake of a bubble rising in a thin-gap cell, J. Fluid Mech., vol. 778, pp. 60-88

Khinast. J. G., Impact of 2-d bubble dynamics on the selectivity of fast gas-liquid reactions, 2001, Aiche Journal, 47:2304–2319.

Kursula , L., Kexel , F., Fitschen , J., Hoffmann , M., Schlüter , M., Unsteady Mass Transfer in Bubble Wakes Analyzed by Lagrangian Coherent Structures in a Flat-Bed Reactor, Processes **2022**, 10, 2686.

Laurini, L., Béteille, A., Fink, G., Herres-Pawlis, S. and Loubière, K., 2023, Reactive Mass Transfer around Isolated Bubbles Rising in a Thin-Gap Cell. Chem. Eng. Technol., 46: 1664-1672

Pavlov, L., Cazin, S., Ern, P., Roig, V., 2021 , Exploration by

Shake-the-Box technique of the 3D perturbation induced by a bubble rising in a thin-gap cell. *Exp Fluids* **62,** 22.

Roig V., Roudet M., Risso F., Billet A.M., 2012, Dynamics of a high-Reynolds-number bubble rising within a thin gap, J. Fluid Mech., vol. 707, pp. 444-466.

Roudet M., Billet A.M., Cazin S., Risso F., Roig V., 2016, Experimental investigation of interfacial mass transfer mechanisms for a confined high-Reynolds-number bubble rising in a thin gap, *AIChE Journal,* DOI: 10.1002/aic.15562

Yang, L., Dietrich, N., Loubière, K., Gourdon, C., Hébrard, G., 2016, Visualization and characterization of gas-liquid mass transfer around a Taylor bubble right after the formation stage in microreactors. Chemical Engineering Science, 143:364–368.

Zhang, Z., Zhang, H., Yuan, X., Yu, K.-T., 2020, Effective uv-induced fluorescence method for investigating interphase mass transfer of single bubble rising in the hele-shaw cell. Industrial & Engineering Chemistry Research, 59(14):6729–6740.